

Accepted Manuscript

Structures and Magnetic Properties of Cyclic Heterometallic Tetranuclear Clusters

Yuan-Ang Liu, Cai-Yun Wang, Mo Zhang, Xue-Qin Song

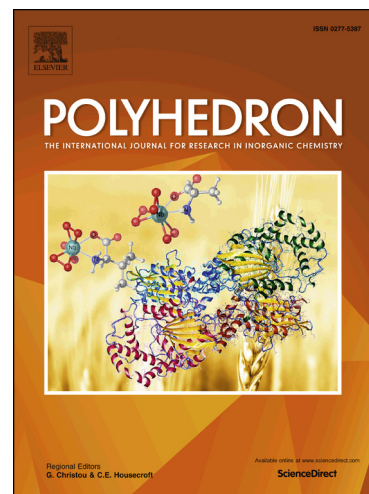
PII: S0277-5387(17)30117-1
DOI: <http://dx.doi.org/10.1016/j.poly.2017.02.007>
Reference: POLY 12474

To appear in: *Polyhedron*

Received Date: 15 January 2017
Revised Date: 8 February 2017
Accepted Date: 8 February 2017

Please cite this article as: Y-A. Liu, C-Y. Wang, M. Zhang, X-Q. Song, Structures and Magnetic Properties of Cyclic Heterometallic Tetranuclear Clusters, *Polyhedron* (2017), doi: <http://dx.doi.org/10.1016/j.poly.2017.02.007>

This is a PDF file of an unedited manuscript that has been accepted for publication. As a service to our customers we are providing this early version of the manuscript. The manuscript will undergo copyediting, typesetting, and review of the resulting proof before it is published in its final form. Please note that during the production process errors may be discovered which could affect the content, and all legal disclaimers that apply to the journal pertain.



Structures and Magnetic Properties of Cyclic Heterometallic Tetranuclear Clusters

Yuan-Ang Liu, Cai-Yun Wang, Mo Zhang, Xue-Qin Song*

School of Chemical and Biological Engineering, Lanzhou Jiaotong University, Lanzhou 730070, Chin

Abstract

A new salicylamide Salen-like multidentate ligand, 1-(2-hydroxy-3-methoxy-benzamido)-2-(2-hydroxy-3-methoxy-benzylideneamino)-ethane (H_3L), was synthesised and used to build up heterometallic magnetic clusters. As a result, four new highly thermal stable cyclic tetranuclear heterometallic clusters which were characterized by elemental analysis, X-ray diffraction, IR and TGA measurements, $[M_2Ln_2L_2(NO_3)_4]$ (M_2Ln_2 , where $M^{II} = Cu^{II}, Ni^{II}$ and $Ln^{III} = Tb^{III}, Dy^{III}$), were successfully obtained with high yield under solvothermal conditions. Temperature-dependent magnetic susceptibility measurements exhibit strong ferromagnetic interactions between Cu^{II} and Ln^{III} in Cu_2Ln_2 which were evaluated by comparing their magnetic susceptibilities with those of the isostructural Ni_2Ln_2 clusters containing diamagnetic Ni^{II} ions. Furthermore, alternating-current magnetic susceptibility studies carried out for the four tetranuclear compounds indicate that Cu_2Ln_2 exhibit interesting slow relaxation of magnetization of the SMM behavior and the effective energy barriers for Cu_2Tb_2 can be obtained from alternating-current susceptibility measurements by applying an external 2000 Oe direct-current field.

Keywords: Salicylamide Salen-like ligand; Heterometallic cluster; Crystal structure; Magnetic properties

1. Introduction

Heterometallic 3d-4f complexes have been gaining increase attention in view of their interesting magnetic properties because they combine the physical characteristics both from transition and lanthanide metal ions with the aid of ingeniously selected organic ligands.[1] There are several

* Corresponding author. Tel.:+86-931-4956619; fax:+86-931-4938755;

E-mail: songxq@mail.lzjtu.cn

advantages in favor of the 3d-4f approach for constructing molecules with SMM behavior: (i) both the large magnetic anisotropy and high spin of the 4f metal ions (particularly Tb^{III} and Dy^{III}) contribute to promote a high U_{eff} ; (ii) unlike in homometallic 4f complexes where exchange coupling is very weak unless promoted by radical ligands,[2] in 3d-4f complexes, effective exchange coupling between 3d and heavy lanthanide centers seems to be possible. This not only stabilizes the bistable ground state but also to some extent suppresses quantum tunneling to provide slow magnetization relaxation. Therefore, the construction of compounds incorporating both transition metal and lanthanide ions represents a promising field of research in molecule-based magnetic materials[3]. Since the first discovery of SMM behavior in 3d-4f complex [4] research into heterometallic complexes has been developed as a significant branch in the field of SMMs with a great deal of 3d-4f complexes, containing Cr-Ln,[5] Mn-Ln,[6] Fe-Ln,[7] Co-Ln,[8] Cu-Ln,[9] Ni-Ln[10] and Zn-Ln [11] behaving as SMMs.

To date, some empirically methodologies to obtain a variety of magnetic heterometallic complexes have been established. In general, the design of ligands containing different coordination donors and bonding modes is considered as a critical factor in determining crystal structure of a heterometallic complex. In addition, some subordinate factors including the nature of anions and the introduction of secondary ligands also play a vital role in the assembly of heterometallic compounds.[12] After carefully surveying literature, we found that Matsumoto and coworkers reported several cyclic $[M^{II}_2Ln^{III}_2]$ tetranuclear complexes by mixing methanolic solutions of $K[Cu^{II}L']$ which exhibits a donor coordination ability and $Ln^{III}(hfac)_3(H_2O)_2$ which shows an acceptor coordination ability in a 1 : 1 mole ratio, where $H_3L' =$ 1-(2-hydroxybenzamido)-2-(2-hydroxy-3-methoxy-benzylideneamino)-ethane and $Hhfac =$ hexafluoroacetylacetone.[13] Their studies have demonstrated that the 3d-4f cyclic tetranuclear structure is a suitable molecular design to generate a large magnetic moment and large magnetic anisotropy, possibly leading to a single molecule magnet. This inspired us to synthesis heterometallic 3d-4f compounds by using a new ortho-methoxy-substituted salicylamide Salen-like ligand toward SMMs based on the followings: The fully deprotonated salicylamide Salen-like ligand has two distinct coordination compartments: one pocket (2N, 2O) suitable for the transition metal (3d) ions and another pocket (4O) suitable for lanthanide (4f) metal ions.

Additionally, the ortho-methoxy-substituted salicylamide group can be utilized for cluster expansion. In this context, four new cyclic tetranuclear heterometallic clusters, $[M_2Ln_2L_2(NO_3)_4]$ (M_2Ln_2 , where $M^{II} = Cu^{II}, Ni^{II}$ and $Ln^{III} = Tb^{III}, Dy^{III}$) were successfully synthesised without using metalloligands under solvothermal conditions. Temperature-dependent magnetic susceptibility measurements exhibit strong ferromagnetic interactions between Cu^{II} and Ln^{III} in Cu_2Ln_2 which were evaluated by comparing their magnetic susceptibilities with those of the isostructural Ni_2Ln_2 clusters containing diamagnetic Ni^{II} ions. Alternating-current magnetic susceptibility studies show that slow relaxation of magnetization were observed in the Cu_2Ln_2 compounds, while no SMM behavior was observed in Ni_2Ln_2 .

2. Experimental

2.1. Materials and instrumentation

Methyl 2-hydroxy-3-methoxybenzoate, 2-hydroxy-3-methoxy-benzaldehyde and ethane-1,2-diamine were obtained from Aladdin. Solvents and all other chemicals were analytical grade, available commercially, and used as received.

Elemental analyses (C, H and N) were performed on a Perkin-Elmer 2400 Series II CHNO elemental analyzer. IR spectra were recorded in the range $400 \sim 4000 \text{ cm}^{-1}$ on a Perkin-Elmer FTIR spectrometer using KBr pellets. X-ray powder diffraction (XRPD) pattern of the samples were recorded on a X-ray diffractometer (Rigaku D/Max 2200PC) with a graphite monochromator and Cu $K\alpha$ radiation ($\lambda = 1.5418 \text{ \AA}$) at room temperature with a scan speed of 0.2 s/step and a step size of 0.02 (2θ), while the voltage and electric current were held at 40 kV and 20 mA.

Thermogravimetric and differential thermal analysis experiments were performed using a TGA/NETZSCH STA449C instrument heated from $27 \sim 800 \text{ }^\circ\text{C}$ under N_2 atmosphere.

Direct-current (dc) magnetic susceptibility measurements were carried out on a Quantum Design SQUID MPMS-XL 7 magnetometer operating between 2 and 300 K for dc applied fields at 1000 Oe. Field dependence of the magnetization at 2K magnetic susceptibility measurements on the polycrystalline samples were performed with the same magnetometer at different magnetic fields. Alternating-current (ac) susceptibility measurements were carried out utilizing an oscillating ac field of 3 Oe and frequencies ranging from 20 to 1600 Hz under 0 and 2000 Oe dc field

respectively. All crystalline samples characterized by PXRD, TG, EA, IR and magnetic studies were obtained from the same batch.

2.2. Synthesis

The synthetic route for H₃L is shown in Scheme 1. N-(2-aminoethyl)-2-hydroxy-3-methoxybenzamide was prepared according to literature using methyl 2-hydroxy-3-methoxybenzoate to replace methyl salicylate.[14] To a 30 mL ethanol solution of N-(2-aminoethyl)-2-hydroxy-3-methoxybenzamide (2.10 g, 10 mmol), 10 mmol (1.52 g) o-Vanilline was added as a solid under stirring. The mixture was refluxed for 4 h to get a clear solution which was then cooled to room temperature. The solution was rotary-evaporated to near dryness to get a pale-yellow solid and the crude product was recrystallized from ethanol to get a bright yellow crystalline product. The crystalline product was washed with diethyl ether and dried in air. H₃L: 3.02 g, Yield 88.0 %. m. p. 155 ~ 156 °C. Analytical data, Calc. for C₁₈H₂₀N₂O₅: C, 62.78; H, 5.85; N, 8.13; Found: C, 62.85, H, 5.86, N, 8.15; IR (KBr, ν , cm⁻¹): 3364 (m), 2998 (w), 1634(s), 1593 (s), 1547 (s), 1468 (s), 1349 (m), 1252 (s), 1066 (m), 969 (m), 914 (m), 837 (m), 776 (m). ¹H NMR (D₆-DMSO, 300 MHz): δ : 3.06 (m, 2H, CH₂), 3.26 (m, 8H, CH₂+2CH₃), 6.23 (m, 2H, ArH), 6.45 (t, 2H, ArH), 6.53 (d, 1H, ArH), 6.83(d, 1H, ArH), 7.98 (s, 1H, CH=N), 8.50 (s, 1H, NH).

General procedure for synthesis of [M₂Ln₂L₂(NO₃)₄]: 0.1 mmol H₃L (0.0345 g) and 0.2 mmol triethylamine (27 μ L) were dissolved in a mixture of 20 mL methanol and 20 mL acetonitrile to obtain a clear yellow solution. Then 0.1mmol Cu(NO₃)₂·3H₂O/Ni(NO₃)₂·6H₂O and Ln(NO₃)₂·6H₂O were added and stirred for 1 h to get a slight turbid brown solution. The turbid brown solution was transferred to three teflon high pressure reactors which maintained at 100 °C for 60 h. After that, the above mixture was cooled to room temperature at a speed of 3 °C/h. Brown crystals suitable for crystal analysis were obtained which were collected by filtration, washed with methanol and dried.

[Cu₂Tb₂L₂(NO₃)₄] (yield: 57.8 mg, 84 % based on Tb(NO₃)₃·6H₂O). Analytical data (%), Calcd: C, 31.43; H, 2.49; N, 8.15; Found: C, 31.57; H, 2.48; N, 8.13; IR (KBr, μ , cm⁻¹): 3424(m), 2925 (m), 2851 (w), 1588(s), 1543 (m), 1472 (s), 1306 (s), 1273 (m), 1235 (m), 1036 (m), 810 (w), 748 (m), 644 (m).

[Cu₂Dy₂L₂(NO₃)₄] (yield: 60.2 mg, 87 % based on Dy(NO₃)₃·6H₂O). Analytical data (%), Calcd: C, 31.27; H, 2.48; N, 8.10; S, 7.00; Found: C, 31.38; H, 2.46; N, 8.11; IR (KBr, μ, cm⁻¹): 3421 (m), 2922 (m), 2851 (w), 1587(s), 1543 (m), 1471 (s), 1306 (s), 1273 (m), 1233 (m), 1038 (m), 812 (w), 747 (m), 644 (m).

[Ni₂Tb₂L₂(NO₃)₄] (yield: 60.1 mg, 88 % based on Tb(NO₃)₃·6H₂O). Analytical data (%), Calcd: C, 31.66; H, 2.51; N, 8.20; Found: C, 31.58; H, 2.52; N, 8.19; IR (KBr, μ, cm⁻¹): 3429(m), 2926 (m), 1587 (s), 1543 (m), 1471 (s), 1406 (s), 1306 (s), 1273 (s), 1038 (m), 953 (m), 812 (w), 750 (m), 644 (m).

[Ni₂Dy₂L₂(NO₃)₄] (yield: 59.0 mg, 86% based on Dy(NO₃)₃·6H₂O). Analytical data (%), Calcd: C, 31.49; H, 2.50; N, 8.16; Found: C, 31.49; H, 2.50; N, 8.17; IR (KBr, μ, cm⁻¹): 3422(m), 2924 (m), 2852 (w), 1587(s), 1543 (m), 1472 (s), 1306 (s), 1273 (m), 1233 (m), 1038 (m), 810 (w), 748 (m), 644 (m).

2.3. X-ray single-crystal diffraction analysis

Suitable brown block crystals of Cu₂Tb₂ (0.32 × 0.29 × 0.26 mm³), Cu₂Dy₂ (0.30 × 0.24 × 0.20 mm³), Ni₂Tb₂ (0.28 × 0.24 × 0.22 mm³) and Ni₂Dy₂ (0.24 × 0.22 × 0.18 mm³) were coated with perfluoropolyether oil before mounting. Intensity data of all four complexes were recorded at 293(2) K employing a Bruker SMART APEX II CCD diffractometer equipped with a monochromatized Mo Kα radiation (λ = 0.71073 Å) source. No crystal decay was observed during the data collections. In all cases, absorption corrections based on multiscans using the SADABS software[15] were applied. The structures were solved by direct methods[16] and refined on F² by a full-matrix least-squares procedure. SHELXL was used for both structure solutions and refinements.[17] All non-hydrogen atoms were refined anisotropically. The positions of hydrogen atoms were calculated and isotropically fixed in the final refinement. The SMART and SAINT software packages[18] were used for data collection and reduction respectively. Crystallographic diagrams were drawn using the DIAMOND software package.[19] A summary of the relevant crystallographic data and the final refinement details are given in Table 1, important bond lengths are listed in Table 2.

3. Results and discussion

3.1 Synthesis and Characterization.

Four M_2Ln_2 cyclic tetranuclear clusters, where $M^{II} = Cu^{II}, Ni^{II}$ and $Ln^{III} = Tb^{III}, Dy^{III}$ were smoothly synthesized in high yields upon reaction of $Cu(NO_3)_2 \cdot H_2O$, $Ln(NO_3)_3 \cdot 6H_2O$, H_3L and NEt_3 in a 1 : 1 : 1 : 2 molar ratio under solvothermal conditions. The four compounds which were found soluble solely in methanol, DMSO and DMF were consistent with their chemical formulas. Consistent with the successful formation of the desired compounds, the characteristic band of carbonyl and imine of the H_3L (1634 and 1593 cm^{-1}) hypochromic shifted about 47 and 50 cm^{-1} , with two new bands presented at IR spectra ca. 1587 cm^{-1} and 1543 cm^{-1} respectively. The absence of band corresponding to the free nitrate groups in the spectra of the compounds implying the absence of free nitrate groups. The bands assigned to the coordinated nitrates were observed as two group bands at about 1471 cm^{-1} (ν_1) and 1306 cm^{-1} (ν_4) and the differences between the strongest absorption band ν_1 and ν_4 of nitrate groups lie in ca 165 cm^{-1} , indicating the existence of bidentate nitrate anions[20] which are further confirmed by X-ray crystallography as follows. Crystalline samples of the four M_2Ln_2 are quite stable at room temperature. TGA have been carried out for four complexes under N_2 atmosphere to show their thermal stability and these four compounds show very similar thermal behavior, therefore we select Cu_2Tb_2 to describe as a representative. As shown in Fig. 1, Cu_2Tb_2 can be stable up to $318\text{ }^\circ\text{C}$ under the protection of nitrogen. After that, the entire architecture began to collapse which might be due to the loss of L^{3-} as well as coordinated nitrates. Clearly, these four clusters did not decompose completely till $800\text{ }^\circ\text{C}$. PXRD experiments were also carried out for the four compounds to confirm whether the crystal structures are truly representative of the bulk materials (Fig. 2). The almost perfect superposition of the experimental PXRD patterns with that calculated from the single crystal study confirmed the phase purity of the bulky samples.

3.2 Crystal structure Descriptions

Single-crystal X-ray diffraction analysis reveal that all four M_2Ln_2 complexes are isostructural tetranuclear compounds which crystallize in a triclinic system in the space group P-1 with $Z = 1$. Detailed structural analysis reveals that the four tetranuclear heterometallic complexes M_2Ln_2 are assembled by the coordination of two fully deprotonated ligands, L^{3-} , and four bidentate nitrate anions as shown in Fig. 3a. In view of their structural similarity, Cu_2Tb_2 has been chosen as a representative example to elucidate the salient structural features. The asymmetric unit of M_2Ln_2

contains one-half of the total molecule, viz., $[M^{\text{II}}\text{Ln}^{\text{III}}\text{L}(\text{NO}_3)_2]$, and the full molecule is generated by the 2-fold axis of rotation (C_2), which passes exactly through the center of the molecule. As depicted in Fig. 3b, each fully deprotonated L^{3-} acted as nonadentate linker holds two different metal ions: Cu^{II} occupies the N_2O_2 pocket from one salicylamide Salen-like ligand to fulfil a square configuration, whereas the oxophilic Tb^{III} is held by the O_9 pocket provided by all oxygen coordination site of L^{3-} in assistance of two bidentate nitrates which is quite different from that of previously reported.[13] In addition, two such $[\text{CuTbL}(\text{NO}_3)_2]$ subunits are tightly held together by carbonyl of salicylamide of two L^{3-} to furnish finally a cyclic core, $[\text{M}_2\text{Ln}_2\text{L}_2(\text{NO}_3)_4]$, which comprises two alternately arrayed transition metal and lanthanide centers. Therefore, within this dinuclear subunit, each L^{3-} adopts a $\mu_3\text{-}\eta_1:\eta_2:\eta_1:\eta_1:\eta_2:\eta_1$ nonadentate coordination mode to hold the three metal centers simultaneously (Fig. 3c). Noticeably, the distance between adjacent Cu^{II} and Ln^{III} is 5.231 and 7.762 Å, respectively. The metric parameters for the Tb^{III} centre was analysed using the SHAPE 2.1 software[21], which revealed that the TbO_9 environments can be described as a distorted monocapped square-antiprism geometry with CShM value of 0.968 for Tb1 (Fig. S1).

3.3 Magnetic Properties

The magnetic susceptibility measurements on the four M_2Ln_2 microcrystalline samples have been performed at 1000 Oe in the 2~300 K temperature range and the data are plotted as $\chi_{\text{M}}T$ versus T in Fig. 4. The $\chi_{\text{M}}T$ values of Cu_2Tb_2 , Cu_2Dy_2 , Ni_2Tb_2 and Ni_2Dy_2 are 23.99, 28.95, 19.56 and 26.41 $\text{cm}^3\cdot\text{mol}^{-1}\cdot\text{K}$ at 300 K respectively. These values are in agreement with the expected theoretical values except that of Ni_2Tb_2 (24.34 $\text{cm}^3\cdot\text{mol}^{-1}\cdot\text{K}$ for Cu_2Tb_2 , 29.09 for Cu_2Dy_2 , 23.64 for and 28.34 for Ni_2Dy_2) for two noninteracting lanthanide ions and two Cu^{II} or Ni^{II} ions. Upon cooling, the $\chi_{\text{M}}T$ products of Cu_2Tb_2 and Cu_2Dy_2 behave similarly with an initial slow increase in $\chi_{\text{M}}T$ which accelerates upon lowering the temperature below 40 K, reaching a maximum value of 75.83 $\text{cm}^3\cdot\text{mol}^{-1}\cdot\text{K}$ for Cu_2Tb_2 and 95.54 $\text{cm}^3\cdot\text{mol}^{-1}\cdot\text{K}$ for Cu_2Dy_2 at 2 K, indicating the existence of ferromagnetic couplings. By comparison, the $\chi_{\text{M}}T$ value for Ni_2Tb_2 is almost constant over the whole temperature range except for a slight increase below 21 K, suggesting weak interactions between the lanthanide ions. This is coincidence with the large Ln–Ln distance of 7.762 Å. Within such long distance, significant magnetic

coupling cannot be induced[22]. As that also depicted in Fig. 4, the $\chi_M T$ value of Ni_2Dy_2 remains almost constant in the temperature range of 300~176 K, and then goes up to a maximum value of $35.22 \text{ cm}^3\cdot\text{mol}^{-1}\cdot\text{K}$ at 19 K, after that, the $\chi_M T$ value decreases to a minimum value of $32.36 \text{ cm}^3\cdot\text{mol}^{-1}\cdot\text{K}$ at 2 K. We could only deduce that the magnetic interactions in Cu_2Ln_2 are stronger than that in Ni_2Ln_2 . As can be seen from crystal analysis, the distance between adjacent Cu^{II} and Ln^{III} is 5.231 and 7.762 Å, which are too long to bring magnetic coupling. In addition, the ligand fields of Ln^{III} in the Cu_2Ln_2 and the Ni_2Ln_2 species may be considered approximately identical as a result of the same valence state and analogous ion radius of Cu^{II} and Ni^{II} . Therefore, the comparison between isomorphous Cu_2Ln_2 and Ni_2Ln_2 complexes, which is defined as a function $\Delta\chi_M T = \chi_M T_{\text{Cu}_2\text{Ln}_2} - \chi_M T_{\text{Ni}_2\text{Ln}_2}$, may eliminate the crystal field contribution of Ln^{III} ions. As shown in Fig. 5, the profile of the $\Delta\chi_M T$ curves in the 2-300 K temperature range exhibit sharp upward trends upon cooling, so we can safely conclude the magnetic interaction between adjacent Cu^{II} and Ln^{III} centers are strong ferromagnetic because square planar Ni^{II} ions are diamagnetic.[23]

The magnetizations vs field for the four cyclic M_2Ln_2 compounds were measured at 2 K which reveal the stronger field dependence of magnetization in Cu_2Ln_2 (the initial rapid increase) than that in compounds Ni_2Ln_2 . As depicted in Fig. 6, the M vs H plots for Cu_2Ln_2 show a sharp rise of magnetization with a steep slope below 4 kOe which is in agreement with the presence of intramolecular ferromagnetic interactions in Cu_2Ln_2 . [24] As for Ni_2Ln_2 , relatively rapid increase in the magnetization below 11 KOe were observed, in accordance with the high-spin state for these complexes, and then moderate increase without achieving a complete saturation at 7 KOe. It should be noted that the magnetization value for Cu_2Tb_2 , Cu_2Dy_2 , Ni_2Tb_2 and Ni_2Dy_2 are $17.75 N\beta$, $18.88 N\beta$, $13.95 N\beta$ and $15.34 N\beta$ respectively. In addition, it is worth mentioning that the M vs H data of the four compounds do not exhibit hysteresis effect at 2 K with sweep rates used ($100\sim 300 \text{ Oe}\cdot\text{min}^{-1}$) which may be caused by the presence of a relatively fast zero-field relaxation as ascertained as follows [24].

In order to study the magnetic dynamics of the four cyclic tetranuclear compounds, variable-temperature ac susceptibility measurements as a function of temperature or frequency were carried out under zero dc field (Fig. 7 and Fig. S2). For Cu_2Ln_2 , the frequency dependence of the in-phase (χ') and out-of phase (χ'') susceptibilities suggests a slow relaxation of the

magnetization which is indicative of the onset of a slow relaxation on the measurement time scale diagnostic of a SMM. However, the χ_M'' peaks are not observed in the temperature ranges available which is mainly due to the presence of fast relaxation of the magnetization by a QTM mechanism through the thermal energy barrier between degenerate energy levels. Therefore, the temperature and frequency dependent ac susceptibility were measured under an applied 2000 Oe field which is depicted in Fig. 8. For the case of Cu_2Tb_2 , the χ_M' shows maximum value which starts to decrease at 4.2 K, while χ_M'' defines a maximum between 2.2 (240 Hz) and 2.6 K (1600 Hz). To confirm whether the relaxation in Cu_2Tb_2 is thermally activated mechanism, the natural log of the relaxations, τ extracted from the peak maxima of χ'' , were plotted versus $1/T$ to check for Arrhenius-type linearity which was normally referred to the Orbach relaxation of the magnetization ($\tau = \tau_0 \exp(U_{\text{eff}}/k_B T)$) (Fig. 9). The best fit of the experimental data to Arrhenius equation $\ln \tau = \ln \tau_0 + U_{\text{eff}}/k_B T$ yielded an energy barrier of $U_{\text{eff}} = 32$ K and $\tau_0 = 1.7 \times 10^{-10}$ s. The relaxation time is consistent with the expected characteristic relaxation times of $10^{-6} \sim 10^{-11}$ s for SMMs.[25] Applying an external field of 2000 Oe for Cu_2Dy_2 , the peaks of χ_M'' signals at various temperatures were shifted to the lower frequency region compared with that of zero field (Fig. 8b). This is also indicative of the reduced QTM effect by applying a external dc field. However, the χ_M'' peaks are still not observed in the temperature ranges available, thus, the energy barriers for magnetization reversal cannot be determined. The observation indicates a more pronounced QTM operates in Cu_2Dy_2 than in Cu_2Tb_2 owing to the Kramers nature of Dy^{III} ion. As shown in Fig. S2, Ni_2Ln_2 showed no frequency-dependent signals of χ_M' and χ_M'' in the same temperature range, demonstrating that the present SMM behavior is not intrinsic to the Ln^{III} centers. It is interesting to compare the magnetic features of Cu_2Tb_2 with those of known $\text{Cu}^{\text{II}}\text{-Tb}^{\text{III}}$ cyclic tetranuclear clusters. The energy barrier for the magnetization reversal of Cu_2Tb_2 of 32 K_B is comparable among the reported $\text{Cu}^{\text{II}}\text{-Tb}^{\text{III}}$ SMMs. It has been shown that the magnetic anisotropy for lanthanide SMM is extremely sensitive to both the local coordination geometry of the lanthanide ion and crystal field effects.[26] Clearly, the replacement of hexafluoroacetylacetonate anions (hfac) with bidentate nitrate anions as well as the introduction of the new fully deprotonated salicylamide Salen-like ligand L^{3-} which shows nonadentate coordination behavior contribute to cause the difference both in the structure and magnetic behavior: in M_2Ln_2 , the coordination polyhedron of

Ln^{III} is distorted monocapped square-antiprism rather than square-antiprism in that previously reported[13]. As a result, the magnetic properties, especially dynamic relaxation behaviors changed accordingly.

Conclusions

Four cyclic heterometallic tetranuclear 3d-4f clusters constructed by a new ortho-methoxy-substituted salicylamide Salen-like ligand with the aid of nitrate anions were prepared in high yield by solvothermal method. This observation bears out the conclusion that the use of solvothermal method is ideal for isolation of the highly thermal stable cyclic tetranuclear 3d-4f clusters without using of metalloligand. In our case, the intramolecular coupling between adjacent Cu^{II} and Ln^{III} centers is strong but have an insignificant impact on the dynamic relaxation, however, the effects of the replacement to the periphery terminal ligands on their magnetic relaxation are obvious, which reveals the feasibility to modulate the magnetic anisotropy of multinuclear 3d-4f SMMs by fine-tuning the local coordination environment.

Appendix A. Supplementary data

CCDC nos. 1524855 ~ 1524858 contains the supplementary crystallographic data for Cu_2Tb_2 , Cu_2Dy_2 , Ni_2Tb_2 and Ni_2Dy_2 . These data can be obtained free of charge via <http://www.ccdc.cam.ac.uk/conts/retrieving.html>, or from the Cambridge Crystallographic Data Centre, 12 Union Road, Cambridge CB2 1EZ, UK; fax: (+44) 1223-336-033; or e-mail: deposit@ccdc.cam.ac.uk.

Acknowledgements

This work was supported by the National Natural Science Foundation of China (Grant 21661099).

References

- [1] a) K. Liu, W. Shi, P. Cheng, *Coord. Chem. Rev.* 289-290 (2015) 74; b) D. I. Alexandropoulos, L. Cunha-Silva, G. Lorusso, M. Evangelisti, J. K. Tang, T. C. Stamatatos, *Chem. Commun.* 52 (2016) 1693; c) S. Schmitz, J. Leusen, N. V. Izarova, Y. H. Lan, W. Wernsdorfer, P. Kögerler, K. Yu. *Dalton Trans.* 45 (2016) 16148.
- [2] a) J. D. Rinehart, M. Fang, W. J. Evans, J. R. Long, *Nat. Chem.* 3 (2011) 538; b) S. Demir, J. M. Zadrozny, M. Nippe, J. R. Long, *J. Am. Chem. Soc.* 134 (2012) 18546; b) M. L. Baker, T. Tanaka, R. Murakami, S. Ohira-Kawamura, K. Nakajima, T. Ishida, H. Nojiri, *Inorg. Chem.* 54 (2015) 5732.

- [3] L. R. Piquer, E. C. Sañudo, Dalton Trans. 44 (2015) 8771.
- [4] S. Osa, T. Kido, N. Matsumoto, N. Re, A. Pochaba, J. Mrozinski, J. Am. Chem. Soc. 126 (2004) 420.
- [5] a) S. K. Langley, D. P. Wielechowski, N. F. Chilton, B. Moubaraki, K. S. Murray, Inorg. Chem. 54 (2015) 10497; b) O. Blacque, A. Amjad, A. Caneschi, L. Sorace, P. -E. Car, New J. Chem. 40 (2016) 3571; c) S. K. Langley, D. P. Wielechowski, B. Moubaraki, K. S. Murray, Chem. Commun. 52 (2016) 10976; d) F. -H. Zhao, S. -H. Liang, S. Jing, Y. Wang, Y. -X. Che, J. -M. Zheng, Inorg. Chem. Commun. 21 (2012) 109; e) X. -Q. Wang, Z. -Y. Li, Z. -X. Zhu, J. Zhu, S. -Q. Liu, J. Ni, J. -J. Zhang, Eur. J. Inorg. Chem. 2013 (2013) 5153.
- [6] a) D. I. Alexandropoulos, T. N. Nguyen, L. Cunha-Silva, T. F. Zafiroopoulos, A. Escuer, G. Christou, T. C. Stamatatos, Inorg. Chem. 52 (2013) 1179; b) H. S. Wang, F. -J. Yang, Q. -Q. Long, Z. -Y. Huang, W. Chen, Z. -Q. Pan, Y. Song, Dalton Trans. 45 (2016), 18221; c) H. Yang, F. Cao, D. Li, S. Zeng, Y. Song, J. Dou, Chem. Eur. J. 21 (2015) 14478; d) T. Yamaguchi, J. -P. Costes, Y. Kishima, M. Kojima, Y. Sunatsuki, N. Bréfuel, J. -P. Tuchagues, L. Vendier, W. Wernsdorfer, Inorg. Chem. 49 (2010) 9125; e) H. Chen, C. -B. Ma, M. -Q. Hu, H. -M. Wen, C. -N. Chen, Dalton Trans. 43 (2014) 16737; f) H. Chen, C. -B. Ma, M. -Q. Hu, H. -M. Wen, H. -H. Cui, J. -Y. Liu, X. -W. Song, C. -N. Chen, Dalton. Trans. 42 (2013) 4908.
- [7] a) D. C. Wilson, S. Liu, X. Chen, E. A. Meyers, X. Bao, A. V. Prosvirin, K. R. Dunbar, C. M. Hadad, S. G. Shore, Inorg. Chem. 48 (2009) 5725; b) D. Visinescu, L. M. Toma, O. Fabelo, C. Ruiz-Pérez, F. Lloret, M. Julve, Inorg. Chem. 52 (2013) 1525; c) J. -L. Liu, J. -Y. Wu, Y. -C. Chen, V. Mereacre, A. K. Powell, L. Ungur, L. F. Chibotaru, X. -M. Chen, M. -L. Tong, Angew. Chem. Int. Edit. 53 (2014) 12966; d) Q. Zhou, F. Yang, D. Liu, Y. Peng, G. Li, Z. Shi, S. H. Feng, Dalton. Trans. 42 (2013) 1039.
- [8] a) J. Goura, A. Chakraborty, J. P. S. Walsh, F. Tuna, V. Chandrasekhar, Cryst. Grow. Des. 15 (2015), 3157; b) S. M. T. Abtab, M. C. Majee, M. Maity, J. Titiš, R. Boča, M. Chaudhury, Inorg. Chem. 53 (2014) 1295; c) S. Hazra, J. Titiš, D. Valigura, R. Boča, S. Mohanta, Dalton Trans. 45 (2016) 7510; d) W. -K. Dong, J. C. Ma, Y. -J. Dong, L. -C. Zhu, Y. Zhang, Polyhedron 115 (2016) 228; e) M. Dolai, M. Ali, J. Titiš, R. Boča, Dalton Trans. 44 (2015) 13242; f) V. Chandrasekhar, S. Das, A. Dey, S. Hossain, S. Kundu, E. Colacio, Eur. J. Inorg. Chem. 2014 (2014) 397; g) L. Zhao, J. F. Wu, S. F. Xue, J. K. Tang, Chem. Asian J. 7 (2012) 2419.
- [9] a) F. J. Kettles, V. A. Milway, F. Tuna, R. Valiente, L. H. Thomas, W. Wernsdorfer, S. T. Ochsenein, M. Murrie, Inorg. Chem. 53 (2014) 8970; b) O. Iasco, G. Novitchi, E. Jeanneau, D. Luneau, Inorg. Chem. 52 (2013) 8723; c) O. Iasco, G. Novitchi, E. Jeanneau, W. Wernsdorfer, D. Luneau, Inorg. Chem. 50 (2011) 7373; d) M. Yang, J. Sun, J. Guo, G. Sun, L. Li, CrystEngComm 18 (2016) 9345; e) W. -W. Kuang, L. -L. Zhu, L. -C. Li, P. -P. Yang, Eur. J. Inorg. Chem. 2015 (2015) 2245; f) J. F. Wu, L. Zhao, M. Guoa, J. K. Tang, Chem. Commun. 51 (2015) 17317; g) S. F. Xue, Y. -N. Guo, L. Zhao, H. X. Zhang, J. K. Tang, Inorg. Chem. 53 (2014) 8165; h) J. F. Wu, L. Zhao, L. Zhang, X. -L. Li, M. Guo, A. K. Powell, J. K. Tang, Angew. Chem.-Int. Ed., 55 (2016) 15574.
- [10] a) S. Biswas, J. Goura, S. Das, C. V. Topping, J. Brambleby, P. A. Goddard, V.

Chandrasekhar, *Inorg. Chem.* 55 (2016) 8422; b) B. Liu, Q. Liu, H. Xiao, W. Zhang, R. Tao, *Dalton Trans.* 42 (2013) 5047; c) K. C. Mondal, G. E. Kostakis, Y. Lan, W. Wernsdorfer, C. E. Anson, A. K. Powell, *Inorg. Chem.* 50 (2011) 11604; d) T. D. Pasatoiu, J. -P. Sutter, A. M. Madalan, F. Z. C. Fellah, C. Duhayon, M. Andruh, *Inorg. Chem.* 50 (2011) 5890; e) W. -K. Dong, J. -C. Ma, L. -C. Zhu, Y. Zhang, *New J. Chem.* 40 (2016) 6998; f) A. Chakraborty, P. Bag, E. Rivière, T. Mallah, V. Chandrasekhar, *Dalton. Trans.* 43 (2014) 8921; g) L. -F. Zou, L. Zhao, Y. -N. Guo, G. -M. Yu, Y. Guo, J. K. Tang, Y. -H. Li, *Chem. Commun.* 47 (2011) 8659; h) L. Zhao, J. F. Wu, H. S. Ke, J. K. Tang, *Inorg. Chem.* 53 (2014) 3519.

[11] a) I. Oyarzabal, B. Artetxe, A. Rodríguez-Diéguez, J. Á. García, J. M. Seco, E. Colacio, *Dalton Trans.* 45 (2016) 9712; b) V. Béreau, H. Bolvin, C. Duhayon, J. -P. Sutter, *Eur. J. Inorg. Chem.* 2016 (2016), 4988; c) X. -Q. Song, P. -P. Liu, Y. -A. Liu, J. -J. Zhou, X. -L. Wang, *Dalton. Trans.* 45 (2016) 8154; d) L. Zhang, L. Zhao, P. Zhang, C. Wang, S. -W. Yuan, J. K. Tang, *Inorg. Chem.* 54 (2015) 11535; e) J. F. Wu, L. Zhao, L. Zhang, X. -L. Li, M. Guo, J. K. Tang, *Inorg. Chem.* 55 (2016) 5514

[12] P. Zhang, L. Zhang, S. -Y. Lin, J. K. Tang, *Inorg. Chem.* 52 (2013) 6595.

[13] a) T. Hamamatsu, K. Yabe, M. Towatari, S. Osa, N. Matsumoto, N. Re., A. Pochaba, J. Mrozinski, J. -L. Gallani, A. Barla, P. Imperia, C. Paulsen, J. -P. Kappler, *Inorg. Chem.* 46 (2007) 4458; b) T. Kido, S. Nagasato, Y. Sunatsuki, N. Matsumoto, *Chem. Commun.* (2000) 2113. c) T. Kido, Y. Ikuta, Y. Sunatsuki, Y. Ogawa, N. Matsumoto, N. Re, *Inorg. Chem.* 42 (2003) 398.

[14] a) X. -Q. Song, P. -P. Liu, Z. -R. Xiao, X. Li, Y. -A. Liu, *Inorg. Chim. Acta.* 438 (2015) 232; b) P. -P. Liu, L. Sheng, X. -Q. Song, W. -Y. Xu, Y. -A. Liu, *Inorg. Chim. Acta.* 434 (2015) 252.

[15] a) SADABS, version 2.03; Bruker AXS Inc. Madison, WI, 2002; b) D. C. Santra, K. B. Manas, K. S. Pradip, M. Sudip, *Chem. Eur. J.* 22 (2016) 2012.

[16] G. M. Sheldrick, *Acta Crystallogr., Sect. A: Found. Crystallogr.* 1990, 46A, 467.

[17] G. M. Sheldrick, *SHELXL-2014*; University of Gottingen: Gottingen, Germany, 2014.

[18] a) SAINT, version 6.02; Bruker AXS Inc. Madison, WI, 2002; b) K. Bhattachary, M. Maity, D. Mondal, A. Endo, M. Chaudhury, *Inorg. Chem.* 51 (2012) 7454.

[19] DIAMOND, Visual Crystal Structure Information System, version 3.1; Crystal Impact: Bonn, Germany, 2004.

[20] a) X. -Q. Song, G. -Q. Cheng, X. -R. Wang, W. -Y. Xu, P. -P. Liu, *Inorg. Chim. Acta.* 425 (2015) 145; b) X. -Q. Song, Y. -K. Lei, X. -R. Wang, M. -M. Zhao, Y. -Q. Peng, G. -Q. Cheng, *J. Solid. State. Chem.* 425 (2014) 202;

[21] A. K. Mondal, H. S. Jena, A. Malviya, S. Konar, *Inorg. Chem.* 55 (2016) 5237.

[22] J. F. Wu, L. Zhao, P. Zhang, L. Zhang, M. Guo, J. K. Tang, *Dalton Trans.* 44 (2015) 11935.

[23] a) B. Q. Ma, S. Gao, G. Su, G. X. Xu, *Angew. Chem., Int. Ed.* 40 (2001) 448; b) A. Figuerola, C. Diaz, J. Ribas, V. Tangoulis, J. Granell, F. Lloret, J. Mahia, M. Maestro, *Inorg. Chem.* 42 (2003) 641; c) J. P. Costes, F. Dahan, A. Dupuis, J. R. Laurent, *Chem. Eur. J.* 4 (1998) 1616; d) A.

Caneschi, L. Sorace, U. Casellato, P. Tomasin, P. A. Vigato, *Eur. J. Inorg. Chem.* 2005 (2005) 3887; e) W. T. Chen, G. C. Guo, M. S. Wang, G. Xu, L. Z. Cai, T. Akits, M. A-. Tanaka, A. Matsushita, J. S. Huang, *Inorg. Chem.* 46 (2007) 2105; f) H. -L. Gao, B. Zhao, X. -Q. Zhao, Y. Song, P. Cheng, D. -Z. Liao, S. -P. Yan, *Inorg. Chem.* 47 (2008) 11057.

[24] P. -H. Lin, T. J. Burchell, R. Clérac, M. Murugesu, *Angew. Chem. Int. Ed.* 47 (2008) 8848.

[25] J. Zhang, H. Zhang, Y. Chen, X. Zhang, Y. Li, W. Liu, Y. Dong, *Dalton Trans.* 45 (2016) 16463.

[26] K. Zhang, C. Yuan, F. -S. Guo, Y. -Q. Zhang, Y. -Y. Wang, *Dalton Trans.* 46 (2017) 186.

Table 1 Crystal data and structure refinement parameters for four M_2Ln_2 compounds

Compound	Cu_2Tb_2	Cu_2Dy_2	Ni_2Tb_2	Ni_2Dy_2
Empirical formula	$Cu_2Tb_2C_{36}H_{34}N_8O_{16}$	$Cu_2Dy_2C_{36}H_{34}N_8O_{16}$	$Ni_2Tb_2C_{36}H_{34}N_8O_{16}$	$Ni_2Dy_2C_{36}H_{34}N_8O_{16}$
M	1375.67	1382.81	1365.95	1373.09
Crystal system,Space group	Triclinic, P-1	Triclinic, P-1	Triclinic, P-1	Triclinic, P-1
$a/\text{\AA}$	7.8697(14)	7.8897(12)	7.9157(12)	7.9159(11)
$b/\text{\AA}$	11.2615(18)	11.2815(16)	11.2498(19)	11.2330(13)
$c/\text{\AA}$	12.875(2)	12.885(12)	12.8344(19)	12.7907(17)
$\alpha/^\circ$	77.940(13)	74.940(13)	77.951(13)	77.923(11)
$\beta/^\circ$	84.356(13)	85.356(16)	84.319(12)	84.351(11)
$\gamma/^\circ$	72.374(15)	73.374(14)	72.085(14)	72.132(11)
$V/\text{\AA}^3, Z$	1062.7(3), 1	1070.3(3)	1062.8(3), 1	1057.8(2), 1
Crystal size (mm)	$0.32 \times 0.29 \times 0.26$	$0.30 \times 0.24 \times 0.20$	$0.28 \times 0.24 \times 0.22$	$0.24 \times 0.22 \times 0.18$
$D_{\text{calcd}}/\text{kg m}^{-3}$	2.150	2.145	2.134	2.155
μ/mm^{-1}	4.373	4.528	4.254	4.467
F(000)	670	672	668	670
θ range for data collection/deg	3.44~ 26.00	3.41~ 26.00	3.455~ 26.00	3.46~ 26.00
Completeness to $\theta = 25.02$	99.7 %	99.7 %	99.7 %	99.7%
index ranges, hkl	-9 \leq h \leq 9 -13 \leq k \leq 13 -15 \leq l \leq 9	-9 \leq h \leq 9 -13 \leq k \leq 13 -15 \leq l \leq 9	-9 \leq h \leq 9 -13 \leq k \leq 13 -15 \leq l \leq 15	-15 \leq h \leq 17 -21 \leq k \leq 19 -22 \leq l \leq 25
R_{int}	0.0474	0.0562	0.0433	0.0349
Reflections collected/unique	7413/ 4164	7456/4208	7396/ 4170	6528 /4140
Data/restraints/params	4164/ 0 / 318	4208/ 0/ 318	4170 / 0 / 318	4140 / 0 /318
Goodness-of-fit on F^2	1.021	1.021	1.035	1.060
Final R indices [$I > 2\sigma(I)$]	$R_I=0.0442, wR_2= 0.0869$	$R_I=0.0446, wR_2= 0.0884$	$R_I=0.0403, wR_2= 0.0747$	$R_I=0.0341, wR_2= 0.0612$
R indices (all data)	$R_I=0.0630, wR_2=0.0970$	$R_I=0.0639, wR_2=0.0988$	$R_I=0.0526, wR_2= 0.0829$	$R_I=0.0414, wR_2= 0.0649$
Largest diff. peak and hole	-1.265 and 1.292 $e.\text{\AA}^{-3}$	-1.222a nd 1.357 $e.\text{\AA}^{-3}$	-0.830 and 1.661 $e.\text{\AA}^{-3}$	-1.681 and 2.16 $e.\text{\AA}^{-3}$

Table 2 Selected bond lengths (\AA) for Cu_2Tb_2 , Cu_2Dy_2 , Ni_2Tb_2 and Ni_2Dy_2 .

[$Cu_2Tb_2L_2(NO_3)_4$]									
Cu1-O3	1.888(4)	Cu1-N1	1.910(5)	Cu1-O2	1.910(4)	Cu1-N2	1.914(5)	Tb1-O4	2.283(4)
Tb1-O3	2.333(4)	Tb1-O2	2.359(4)	Tb1-O9	2.429(5)	Tb1-O10	2.456(4)	Tb1-O6	2.471(5)
Tb1-O7	2.521(5)	Tb1-O5	2.554(4)	Tb1-O1	2.567(4)				
[$Cu_2Dy_2L_2(NO_3)_4$]									
Cu1-O2	1.893(4)	Cu1-N2	1.896(5)	Cu1-O4	1.928(5)	Cu1-N1	1.951(6)	Dy1-O5	2.577(4)
Dy1-O1	2.574(4)	Dy1-O10	2.559(5)	Dy1-O9	2.459(5)	Dy1-O7	2.453(4)	Dy1-O6	2.417(5)
Dy1-O2	2.405(5)	Dy1-O4	2.316(4)	Dy1-O3	2.266(4)				
[$Ni_2Tb_2L_2(NO_3)_4$]									
Ni1-N2	1.842(5)	Ni1-O2	1.847(4)	Ni1-N1	1.855(5)	Ni1-O4	1.868(4)	Tb1-O3	2.282(4)
Tb1-O2	2.341(4)	Tb1-O4	2.363(4)	Tb1-O6	2.433(4)	Tb1-O7	2.448(5)	Tb1-O10	2.463(5)
Tb1-O9	2.510(4)	Tb1-O1	2.528(4)	Tb1-O5	2.537(4)				
[$Ni_2Dy_2L_2(NO_3)_4$]									
Ni1-N2	1.835(4)	Ni1-O2	1.849(3)	Ni1-N1	1.853(3)	Ni1-O4	1.856(3)	Dy1-O3	2.266(3)
Dy1-O2	2.329(3)	Dy1-O4	2.355(3)	Dy1-O9	2.416(4)			Dy1-O6	2.454(3)
Dy1-O7	2.512(3)	Dy1-O1	2.517(3)	Dy1-O5	2.523(3)				

Scheme. 1 The synthetic route of the ligand L

Fig. 1 TGA curves of Cu_2Tb_2 .

Fig. 2 Powder X-ray diffraction patterns of the four M_2Ln_2 complexes.

Fig. 3 (a) Molecular structure of Cu_2Tb_2 (Hydrogen atoms have been omitted for clarity). (b) The asymmetric unit of Cu_2Tb_2 with thermal ellipsoids at 30% probability. (c) Coordination mode of fully deprotonated L^{3-} in Cu_2Tb_2 . Color scheme: Tb atoms, green; C atoms, gray; O atoms, red; N atoms, blue; Cu atoms, brown.

Fig. 4 Temperature dependence of magnetic susceptibilities in the form of $\chi_M T$ vs. T for M_2Ln_2 at 1 kOe.

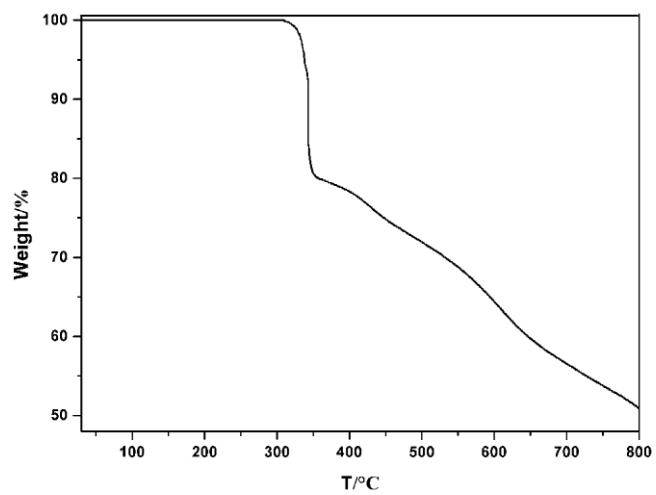
Fig. 5 $\Delta\chi_M T$ for M_2Ln_2 at 1 kOe.

Fig. 6 The magnetizations versus field plots for M_2Ln_2 at 2 K.

Fig. 7 Frequency dependence of the in phase (χ_M') and out-of-phase (χ_M'') susceptibility at different temperature without dc field for Cu_2Ln_2 .

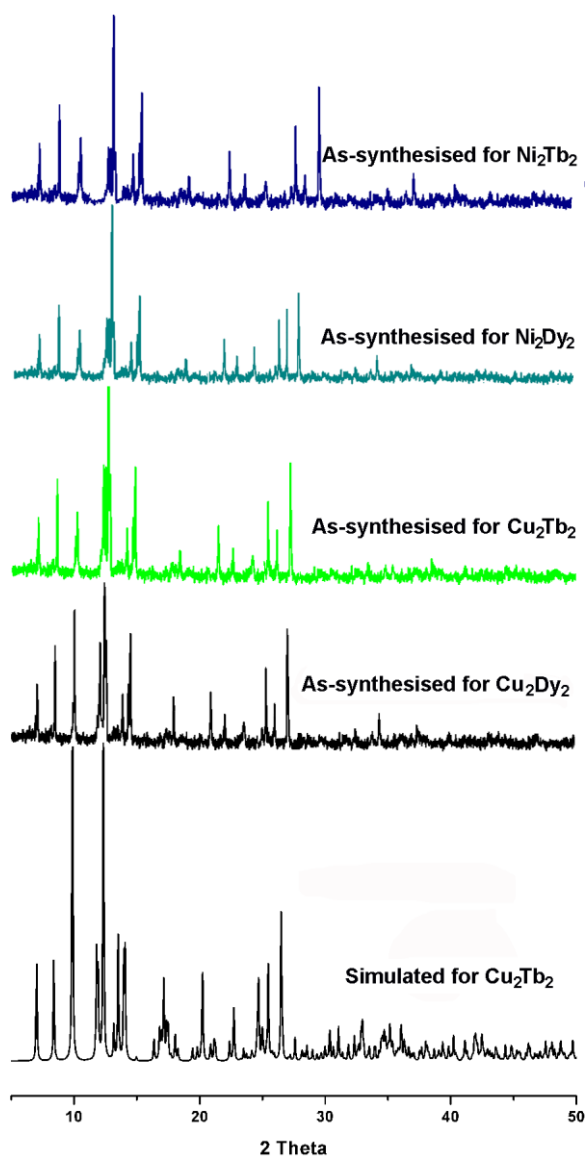
Fig. 8 Frequency dependence of the in phase (χ_M') and out-of-phase (χ_M'') susceptibility at different temperature and 2000 Oe dc field for Cu_2Ln_2 .

Fig. 9 $\ln \tau$ versus T^{-1} plots for Cu_2Tb_2 . The red line represents the fit to the Arrhenius law.

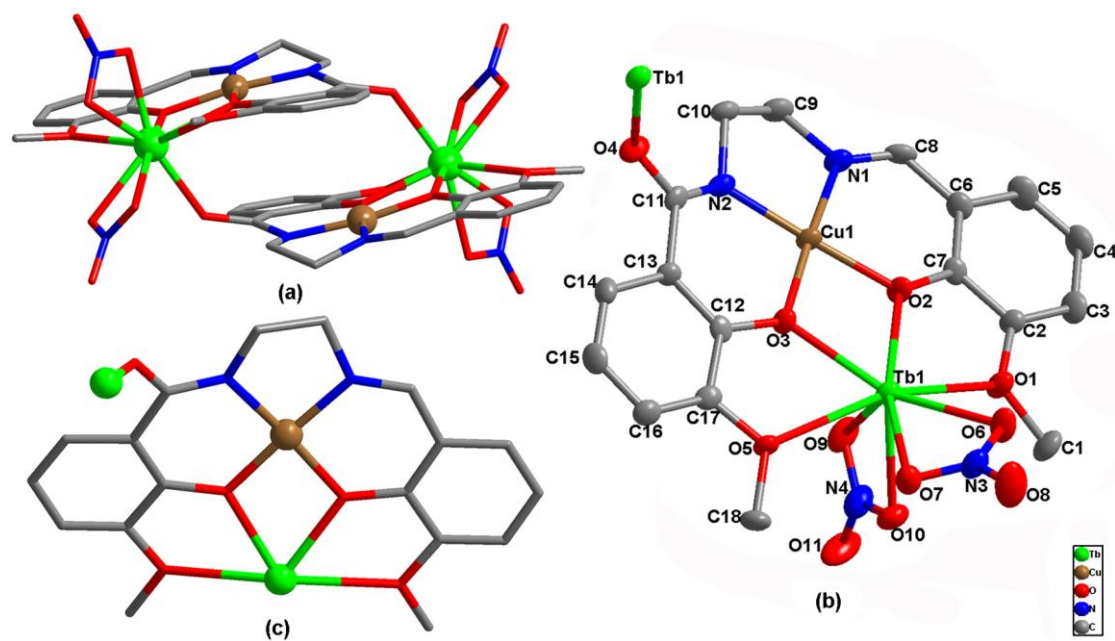


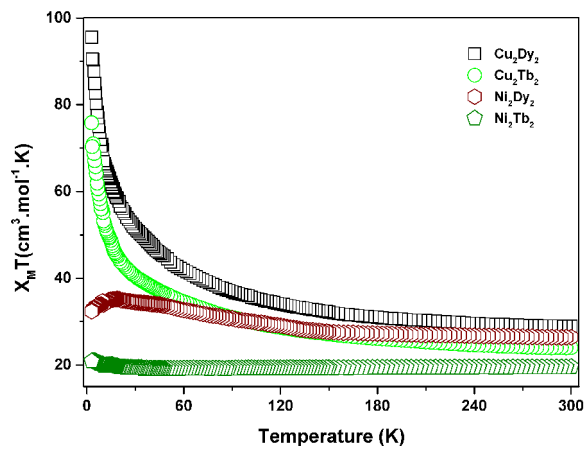
↑

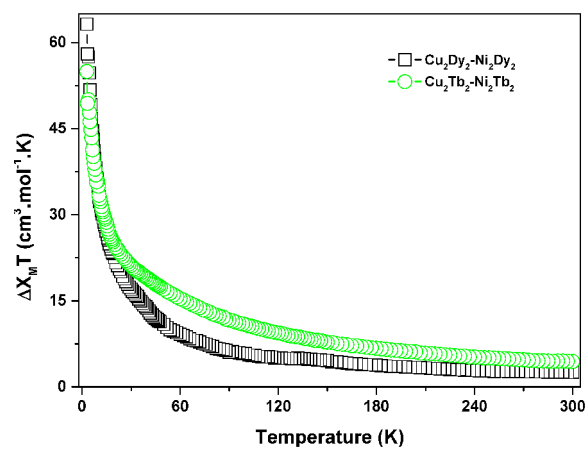
ACCEPTED MANUSCRIPT

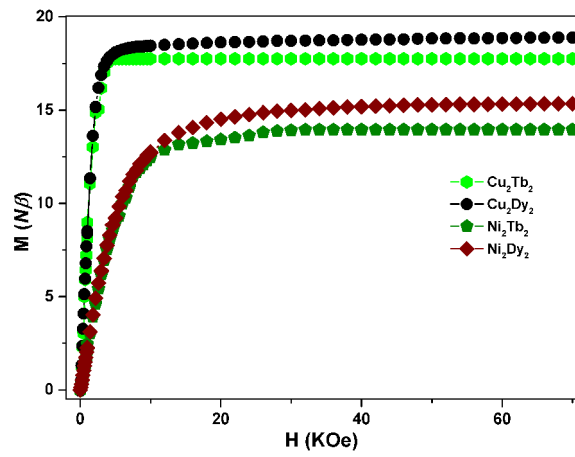


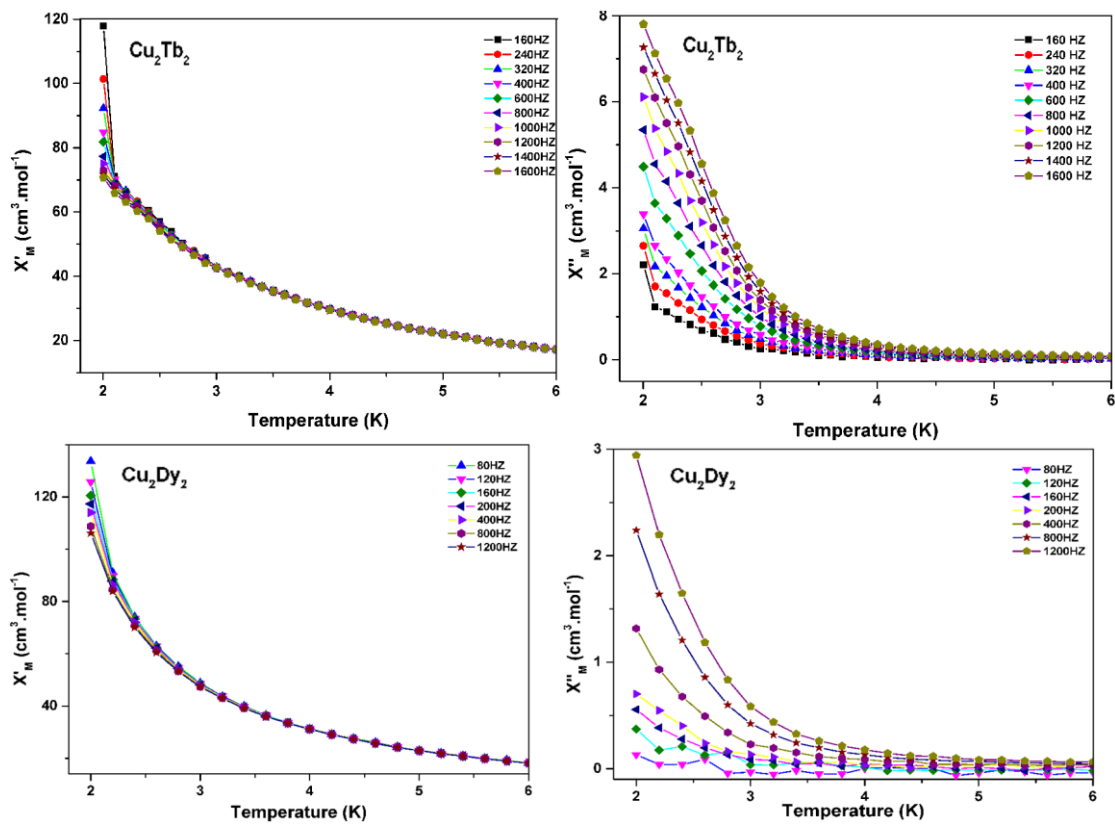
ACCEPTED

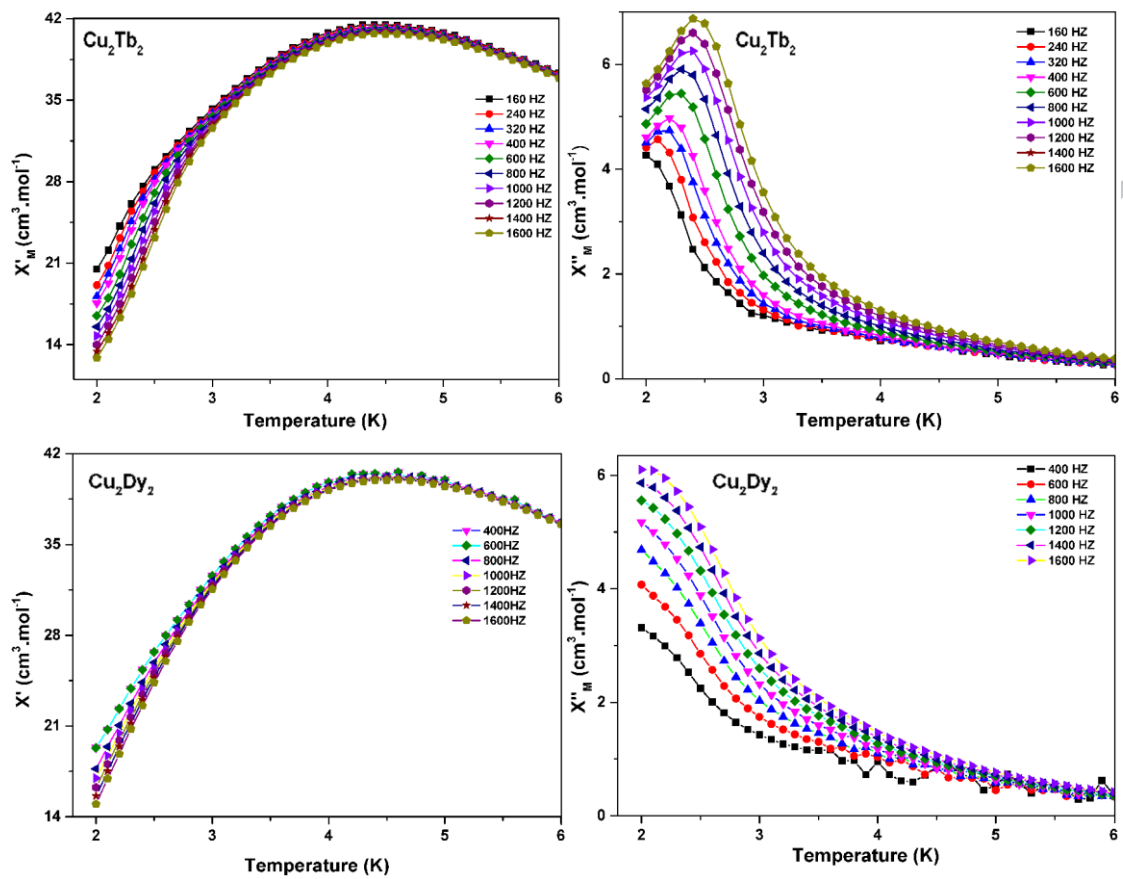


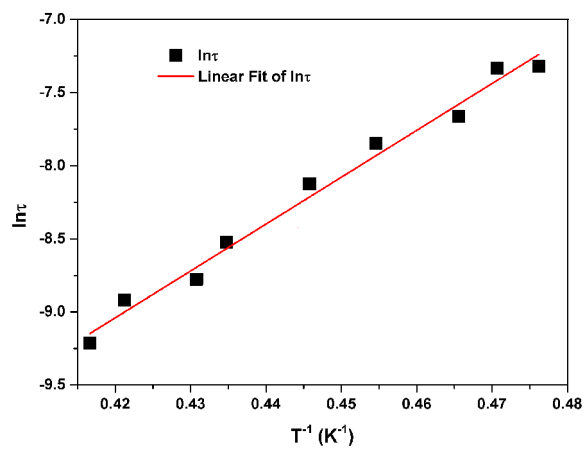


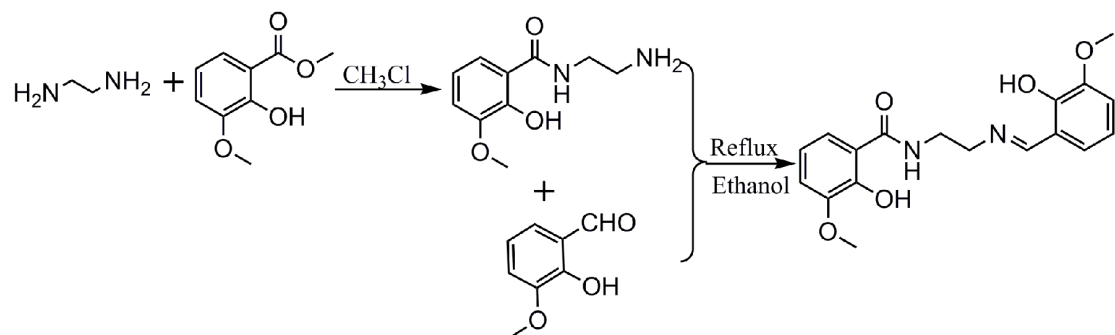












We present here four new highly thermal stable cyclic tetranuclear heterometallic clusters which exhibit interesting magnetic behaviors.

